Collective Expansion in Central Au + Au Collisions

W. C. Hsi,[1] G. J. Kunde,[2] J. Pochodzalla,[2] W. G. Lynch,[1] M. B. Tsang,[1] M. L. Begemann-Blaich,[4] D. R. Bowman,[1,*] R. J. Charity,[3] F. Cosmo,[5] A. Ferrero,[6,†] C. K. Gelbke,[1] T. Glasmacher,[1] T. Hofmann,[2] G. Imme,[7] I. Iori,[6] J. Hubele,[2] J. Kempter,[4] P. Kreutz,[4] W. D. Kunze,[2] V. Lindenstruth,[2] M. A. Lisa,[1,‡] U. Lynen,[2] M. Mang,[4] A. Moroni,[6] W. F. J. Müller,[2] M. Neumann,[4] B. Ocker,[4] C. A. Ogilvie,[2,§] G. F. Peaslee,[1,**] G. Raciti,[7] F. Rosenberger,[4] H. Sann,[2] R. Scardaoni,[6] A. Schüttauf,[4] C. Schwarz,[1] W. Seidel,[8] V. Serfling,[4] L. G. Sobotka,[3] L. Stuttge,[5] S. Tomasevic,[5] W. Trautmann,[2] A. Tucholski,[9] C. Williams,[1] A. Wörner,[2] and B. Zwieglinski[9]

[1]*Department of Physics and Astronomy and National Superconducting Cyclotron Laboratory, Michigan State University, East Lansing, Michigan 48824*

[2]*Gesellschaft für Schwerionenforschung, D-64220, Darmstadt, Germany*

[3]*Department of Chemistry, Washington University, St. Louis, Missouri 63130*

[4]*Institut für Kernphysik, Universität Frankfurt, D-60486, Frankfurt, Germany*

[5]*Centre de Recherches Nucléaires, Strasbourg, France*

[6]*INFN and Dipartimento di Fisica, Università degli Studi di Milano, I-20133, Milano, Italy*

[7]*INFN and Dipartimento di Fisica dell' Università, I-95129, Catania, Italy*

[8]*FZ Rossendorf, D-01314 Dresden, Germany*

[9]*Soltan Institute for Nuclear Studies, Hoza 69, 00-681 Warsaw, Poland*

(Received 29 April 1994)

Energy spectra for intermediate mass fragments produced in central Au + Au collisions at E/A = 100 MeV indicate a collective expansion at breakup. For the first time, values for this collective expansion energy per nucleon are extracted independently for each charge. Typically, these values are one-third to one-half of the incident kinetic energy per nucleon in the c.m. system, but they decrease with Z_f, suggesting that all fragments do not participate equally in the collective expansion.

PACS numbers: 25.70.Pq, 25.70.Gh

Investigations of central nucleus-nucleus collisions reveal that the multiplicity of intermediate mass fragments (IMF's: $Z_f = 3-30$) increases with incident energy to a maximum at $E_{\text{beam}}/A \approx 100$ MeV and declines thereafter [1,2]. Such observations are qualitatively consistent with the excitation energy dependences of statistical models [3–5] and nuclear phase transitions [3,4,6,7]. At $E/A \geq 100$ MeV, dynamical models [8,9], however, predict the fragment multiplicities to be strongly influenced by a rapid expansion from supranormal densities achieved early in the nuclear collision [8], and experimental evidence now suggests a significant collective "radial" expansion [10–13]. This collective expansion may persist to lower incident energies where sidewards directed flow [14–16] vanishes [17,18] due to cancellations between the attractive and repulsive deflections that result from mean field attraction and nucleon-nucleon collisions, respectively. Like measurements of directed transverse flow [14–16], measurements of radial flow [10,13] can provide unique constraints on nuclear transport properties such as the nuclear equation of state [19].

To investigate collective expansion in Au + Au collisions at energies where fragment multiplicities are maximal, thin ^{197}Au targets of 3 and 5 mg/cm^2 areal density were bombarded at the semiconductor-insulator-semiconductor (SIS) facility of Gesellschaft für Schwerionenforschung Darmstadt m.b.H. (GSI) by ^{197}Au ions of E/A = 100 and 400 MeV incident energy. Charged particles emitted to $\theta_{\text{lab}} = 14°-160°$ were detected in 215 plastic-scintillator–CsI(Tl) phoswich detectors of the Miniball/Miniwall [20]. Particles which penetrated the plastic-scintillator foils of these phoswich detectors were identified by element for $Z \leq 10$ and by isotope for $Z = 1$ and 2. For $25° \leq \theta_{\text{lab}} \leq 160°$, 4 mg/cm^2 plastic-scintillator foils were used, leading to energy thresholds for particle identification of $E_{\text{th}}/A \sim 1.5$ MeV (2.5 MeV) for $Z = 3$ ($Z = 10$) particles, respectively. For $14° \leq \theta_{\text{lab}} \leq 25°$, 8 mg/cm^2 plastic foils were used, leading to energy thresholds of $E_{\text{th}}/A \sim 2.2$ MeV (4.5 MeV) for $Z = 3$ ($Z = 10$) particles, respectively. Lower energy particles with 10 MeV $\leq E \leq E_{\text{th}}$ and $Z \geq 3$ were detected but not identified and were included in the measured charged particle multiplicity N_C. Energy calibrations, accurate to 10%, were obtained for $25° \leq \theta_{\text{lab}} \leq 160°$ by combining the "punchthrough" points measured in this experiment with detailed detector response functions measured at the NSCL K1200 Cyclotron of Michigan State University [21].

Radial flow effects should be enhanced for central collisions [19]; therefore a "reduced" impact parameter, $\hat{b} = b/b_{\text{max}}$, was determined by assuming [1,22,23] that the charged particle multiplicity decreases monotonically with impact parameter. [Here, b_{max} was defined by $\langle N_C(b_{\text{max}})\rangle = 4$.] Laboratory energy spectra for boron fragments from near central collisions ($\hat{b} < 0.33$) display exponential slopes that become steeper with scattering angle; see Fig. 1. Such spectra have been well described at lower incident energies [24,25] and for mass

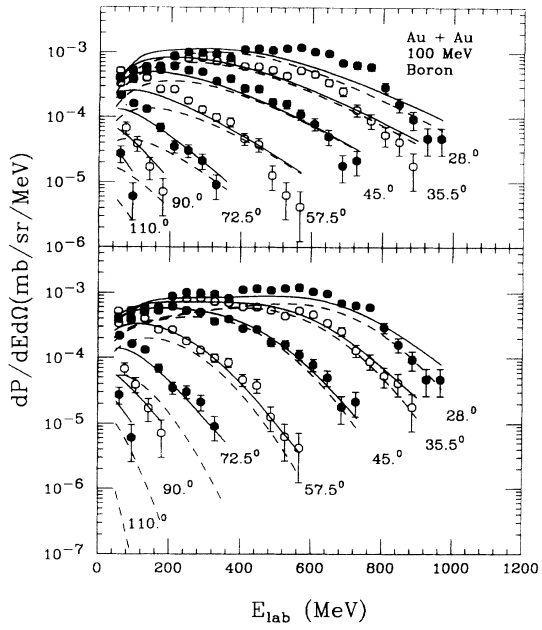

FIG. 1. Comparisons of the energy spectra for boron fragments emitted to $\Theta_{\rm lab} = 28°$, 35.5°, 45°, 57.5°, 72.5°, 90°, and 110° (solid and open points) with corresponding moving source fits. Upper panel: The solid lines correspond to fits obtained with Eq. (1) and no radial expansion. Lower panel: The solid lines correspond to fits obtained with Eqs. (1) and (4), incorporating a radial expansion. The dashed lines in both panels correspond to the respective contributions from the participant sources alone.

asymmetric systems [26] by a superposition of three isotropically emitting thermal sources corresponding to the decay of a participant region formed by the overlap of the projectile and target as well as the decay of remnant projectilelike and targetlike spectator nuclei.

The solid lines in the upper panel in Fig. 1 indicate best fits to the energy spectra assuming three relativistic Maxwellian distributions [27],

$$\frac{dP(\vec{p})}{dE\,d\Omega} = \sum_{i=1}^{3}\frac{dP_i(\vec{p})}{dE\,d\Omega} = \frac{dP_1}{dE\,d\Omega}(\vec{p},\vec{v}_1,V_1) + \int_0^{2\pi}\frac{d\phi_R}{2\pi}\sum_{i=2}^{3}\frac{dP_i}{dE\,d\Omega}(\vec{p},\vec{v}_i(\phi_R),V_i), \quad (1)$$

where E and $\vec{p}$ denote the kinetic energy and momentum of the emitted particle, $\vec{v}_i$ denotes the velocity, V_i denotes the effective Coulomb barrier of the ith source, and ϕ_R denotes the azimuthal angle of the reaction plane [28]. Here, $dP_i/dE\,d\Omega(\vec{p},0,V_i)$ is defined *in the rest frame* of the source ($\vec{v}_i \equiv 0$) by

$$\frac{dP_i}{dE\,d\Omega}(\vec{p},0,V_i) = a_i\Theta(E - V_i)(E + mc^2 - V_i) \times \sqrt{(E + mc^2 - V_i)^2 - m^2c^4} \times \exp\left(-\frac{E - V_i}{T_i}\right), \quad (2)$$

and $dP_i/dE\,d\Omega(\vec{p},\vec{v}_i,V_i)$ *is obtained from Eq.* (2) *by Lorentz transformation.* In Eq. (2), a_i is a normalization constant, T_i is a temperature parameter, $\Theta(E - V_1)$ is the unit step function, and mass m is taken from that for the most abundant natural isotope, e.g., $A = 11$ for boron. Because of the mass symmetry of the entrance channel, $\vec{v}_3 = -\vec{v}_2$, $a_3 = a_2$, and $T_3 = T_2$ is stringently required in the c.m. frame for the spectator sources. The transverse velocities of the spectator sources ($i = 2, 3$) were determined from fits to triple differential cross sections measured with respect to the reaction plane [29]; they influence little the parameters of the participant source given in Table I.

Contributions from the participant source (dashed lines) dominate the fits at $\theta_{\rm lab} = 35.5°$ and 45°. Spectator sources, indicating undamped longitudinal collective motion, contribute strongly at backward angles and for very high energies at forward angles but not at $28° \le \theta_{\rm lab} \le 57.5°$ for 400 MeV $\le E_{\rm lab} \le$ 700 MeV, where the shapes of the measured spectra are very poorly described by thermal source fits. Similar difficulties are encountered for the energy spectra of other IMF's with $3 \le Z_f \le 6$.

The impact parameter gate, $\hat{b} < 0.33$, includes noncentral collisions with large angular momentum. Thus, "rotational" flow (due to the nuclear mean field attraction [30,31]) and repulsive transverse collective flow can influence the momentum and energy distributions. Such effects will be reflected in azimuthally anisotropic emission patterns [15,16,30,31] and revealed by constructing α-α azimuthal angular correlation functions, $1 + R(\Delta\phi_{\alpha\alpha})$, defined by

$$\sum Y_2(\vec{p}_1,\vec{p}_2) = [1 + R(\Delta\phi_{\alpha\alpha})]\sum Y_1(\vec{p}_1)\sum Y_1(\vec{p}_2). \quad (3)$$

Here, Y_1 and Y_2 are the singles and coincidence yields, $\vec{p}_1$ and $\vec{p}_2$ are the momenta for the particles 1 and 2, and $\Delta\phi_{\alpha\alpha} = \phi_{\alpha_1} - \phi_{\alpha_2}$ is the relative azimuthal angle between the two alpha particles about the beam axis. Both sides of Eq. (3) are summed over momenta $\vec{p}_1$ and $\vec{p}_2$ for fixed $\Delta\phi_{\alpha\alpha}$, subject to an energy threshold of $E/A >$ 10 MeV and common centrality and rapidity gates.

As shown in Fig. 2, evidence for directed flow is observed in correlations near target rapidity at $E/A = 100$ MeV (solid circles). Near midrapidity, however, α-α correlations at $E/A = 100$ (open circles) *are*

TABLE I. Parameters for three-source fits. (Fits 1 and 2 are without and with expansion, respectively, and the units for a_i, T_i, and V_i are MeV^{-3} sr^{-1}, MeV, and MeV, respectively.

Fit	Source	a_i	T_i	$v_{x,i}/c$	$v_{z,i}/c$	V_i	$\beta_{\rm exp}$
1	1	9.1×10^{-11}	70.1	0	0	35	0
	2	6.5×10^{-11}	35.5	0.06	0.12	13	0
2	1	8.9×10^{-10}	16.6	0	0	0	0.15
	2	5.8×10^{-11}	35.3	0.06	0.13	13	0

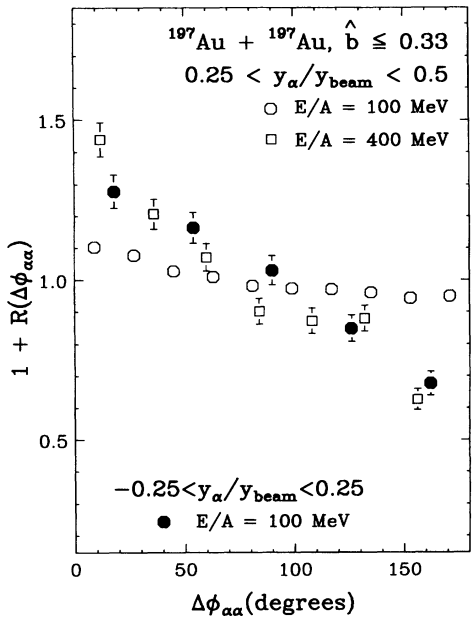

FIG. 2. The open squares designate the measured α-α correlations obtained for central collisions at $E/A = 400$ MeV and $0.25 \leq y_\alpha/y_{\text{beam}} \leq 0.5$. The open circles designate the corresponding α-α correlations for central collisions at $E/A = 100$ MeV. The solid circles designate the α-α correlations for central collisions at $E/A = 100$ MeV and $-0.25 \leq y_\alpha/y_{\text{beam}} \leq 0.25$.

significantly reduced, ruling out large azimuthal anisotropies near midrapidity. These observations stand in contrast to the midrapidity α-α azimuthal correlations observed in central Au + Au collisions at $E/A = 400$ MeV (open squares), where sidewards directed flow is strongly manifested.

Thus for collisions at $E/A = 100$ MeV, collective motion at midrapidity is not strongly correlated with the reaction plane. To determine whether the discrepancies shown in the upper panel of Fig. 1 can be explained by a collective radial flow, a self-similar radial expansion, $\vec{v}(\vec{r}) = c\beta_{\text{exp}}\vec{r}/R_S$, of a spherical participant source [$i = 1$ in Eq. (1)] was assumed which attains its maximum velocity $c\beta_{\text{exp}}$ at the surface $r = R_S$. The velocities of individual particles were assumed to be thermally distributed with temperature T_1 about the local radial expansion velocity. Coulomb expansion after breakup was modeled in the limit of large β_{exp}, i.e., particles with charge Z_f, emitted from a source with charge Z_S, were assumed to gain a kinetic energy $\Delta E_{\text{Coul}}(r) = Z_f(Z_S - Z_f)e^2r^2/R_S^3$, without changing direction. In the c.m. frame one obtains

$$\frac{dP_1}{dE\,d\Omega} = \frac{3}{4\pi R_S^3}\int_0^{R_S} r^2 dr \int d\Omega_r \int dE' \times \frac{dP_1}{dE'\,d\Omega}(\vec{p}\,', \vec{v}(\vec{r}), 0)) \times \delta(E' - E + \Delta E_{\text{Coul}}(r)), \quad (4)$$

with the direction of the particle's momentum assumed unchanged by Coulomb acceleration. The total energy spectrum is obtained by inserting Eq. (4) into Eq. (1) as the participant source.

Best fits, assuming Eq. (4), $Z_S = 118$ and $R_S = 11$ fm, are shown by the solid lines in the lower panel of Fig. 1; the inclusion of collective expansion changes the curvatures of the calculations so as to accurately follow the curvatures of the energy spectra at $28° \leq \theta_{\text{lab}} \leq 57.5°$ where the participant source dominates. Extracted values for β_{exp} are not very sensitive to the temperature T_1, changing by about $\pm 10\%$ with T_1 for 5 MeV $\leq T_1 \leq$ 20 MeV where reasonable fits were obtained. Similar values of β_{exp} for the different Z_f's are extracted (left panel, Fig. 3) for fixed $T_1 = 15$ MeV (solid points), as for when T_1 is varied freely (open points); however, β_{exp} decreases with Z_f suggesting that heavier fragments may not participate as fully as the lighter fragments in the collective expansion. Such an effect could arise if heavier fragments originated from the more dense central regions of the expanding system. Values for β_{exp} are not significantly changed by making a more restrictive gate, $\hat{b} < 0.16$, on the impact parameter.

Since β_{exp} and the Coulomb expansion dynamics have a similar influence on the energy spectra, there is a $\pm 5\%$ variation in β_{exp} with R_S or equivalently the breakup density $\rho_B \approx \rho_0(7.4\text{ fm}/R_S)^3$ over the range $0.1 \leq \rho_B/\rho_0 \leq 0.3$. The mean total radial collective energy, defined by $\langle E_r\rangle = \frac{3}{5}[\frac{1}{2}mc^2\beta_{\text{exp}}^2 + Z_f(Z_S - Z_f)e^2/R_S]$ and shown by the solid points in the right panel of Fig. 3, is considerably less sensitive to ρ_B. Here, $\langle E_r\rangle$ increases with mass (charge) but not linearly as expected for a uniform participation of these fragments in the radial expansion. The radial energies for heavier fragments with $Z_f \geq 5$ increase

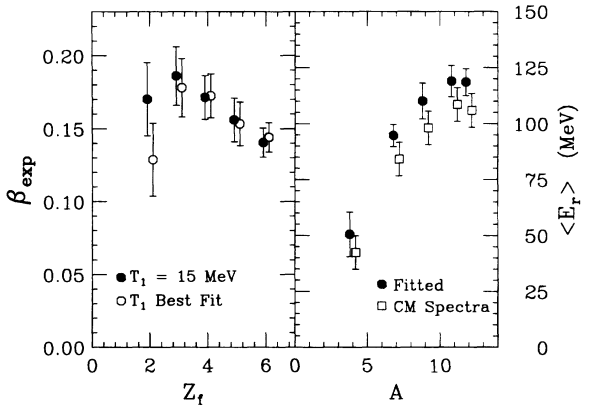

FIG. 3. Left panel: The open points correspond to best fit values for the radial expansion velocities as a function of the fragment charge. The solid points are the corresponding values obtained when T_1 is constrained to be 15 MeV. Right panel: The solid points depict the dependence of the mean radial collective energy $\langle E_r\rangle$ extracted from the fits upon the fragment mass. The open squares depict the corresponding values extracted from Fig. 4 assuming $T_1 = 15$ MeV. Both values are plotted at the mass of the most abundant natural isotope.

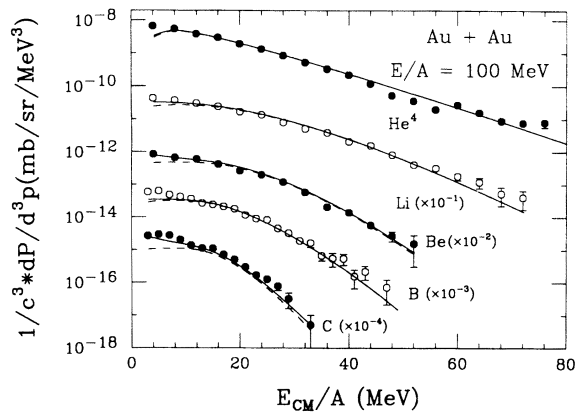

FIG. 4. Energy spectra in the c.m. frame for various fragments detected at $\theta_{c.m.} = 90° \pm 10°$. The solid lines correspond to the three-source fit assuming a radial expansion. The dashed lines depict the participant source alone.

less than one would expect if a linear dependence were followed.

To further support these conclusions, energy spectra in the total c.m. frame at $\theta_{c.m.} = 90°$ are shown in Fig. 4 for $Z_f = 2-6$. The total fit and the participant source only are represented by the solid and dashed lines, respectively. Assuming a temperature $T_1 = 15$ MeV, the mean radial collective energy was independently estimated by integrating these spectra and subtracting the mean thermal kinetic energy of a Maxwell gas, i.e., $\langle E_r \rangle = \langle E \rangle - \frac{3}{2}T_1$. These estimates for $\langle E_r \rangle$ (open squares, right panel of Fig. 3) are somewhat smaller than the fitted values for the participant source (solid points), reflecting additional low energy spectral contributions from the spectator sources. Differences between the solid and open points provide indications of the systematic uncertainties in extracting mean radial kinetic energies for the participant source alone.

In summary, energy spectra for IMF's produced in central Au + Au collisions at $E/A = 100$ MeV indicate large radial collective expansion velocities at breakup. The radial expansion energies, $E_r/A = 8.3-13.5$ MeV, decrease with the fragment charge, but are relatively insensitive to assumptions about the density of the system at breakup, contributions from transverse flow or from the breakup of projectile and target spectator matter. Similar to other results recently obtained [10], the extracted collective energy represents one-third to one-half of the incident kinetic energy per nucleon in the c. m. frame, emphasizing the importance of this new aspect of collective flow and suggesting that expansion may, indeed, play a critical role in the large fragment multiplicities observed.

This work is supported by the National Science Foundation under Grants No. PHY-90-15255 and No. PHY-92-14992 and the U.S. Department of Energy under Contract No. DE-FG02-87ER-40316. J. P. acknowledges the support of the DFG under Contract No. Po 256/2-1.

*Present address: Chalk River Laboratories, Chalk River, Ontario K0J 1J0, Canada.
†On leave from the Comision Nacional Energia Atomica, Argentina.
‡Present address: Lawrence Berkeley Laboratory, Berkeley, CA.
§Present address: Department of Physics, MIT, Cambridge, MA 02139.
**Present address: Physics Department, Hope College, Holland, MI.

[1] M. B. Tsang *et al.*, Phys. Rev. Lett. **71**, 1502 (1993).
[2] G. F. Peaslee *et al.*, Phys. Rev. C **49**, R2771 (1994).
[3] D. H. E. Gross *et al.*, Phys. Rev. Lett. **56**, 1544 (1986).
[4] J. P. Bondorf *et al.*, Nucl. Phys. **A444**, 460 (1986).
[5] W. A. Friedman, Phys. Rev. C **42**, 667 (1990).
[6] J. E. Finn *et al.*, Phys. Rev. Lett. **49**, 1321 (1982).
[7] P. J. Siemens, Nature (London) **305**, 410 (1983).
[8] G. Peilert *et al.*, Phys. Rev. C **39**, 1402 (1989); G. Peilert *et al.*, Phys. Rev. C **46**, 1457 (1992).
[9] D. H. Boal and J. N. Glosli, Phys. Rev. C **38**, 1870 (1988).
[10] S. G. Jeong *et al.*, Phys. Rev. Lett. **72**, 3468 (1994).
[11] H. W. Barz *et al.*, Nucl. Phys. **A531**, 453 (1991).
[12] W. Bauer *et al.*, Phys. Rev. C **47**, 1838 (1993).
[13] R. T. de Souza *et al.*, Phys. Lett. **300B**, 29 (1993).
[14] H. H. Gutbrod, A. M. Poskanzer, and H. G. Ritter, Rep. Prog. Phys. **52**, 1267 (1989).
[15] H. H. Gutbrod *et al.*, Phys. Lett. **216B**, 267 (1989); H. H. Gutbrod *et al.*, Phys. Rev. C **42**, 640 (1990).
[16] Y. Leifels *et al.*, Phys. Rev. Lett. **71**, 963 (1993).
[17] C. A. Ogilvie *et al.*, Phys. Rev. C **42**, R10 (1990).
[18] G. D. Westfall *et al.*, Phys. Rev. Lett. **71**, 1986 (1993). Systematics in this paper suggest a "balance energy" below $E/A = 70$ MeV for the Au + Au system.
[19] Pawel Danielewicz and Qiubao Pan, Phys. Rev. C **46**, 2004 (1992).
[20] R. T. de Souza *et al.*, Nucl. Instrum. Methods Phys. Res., Sect. A **295**, 109 (1990). The Miniwall, a granular extension of the Miniball to forward scattering angles, uses technologies developed for the Dwarf Wall/Ball.
[21] C. Schwarz *et al.*, in National Superconducting Cyclotron Laboratory Annual Report, 1994; similarly accurate response function information for Miniwall detectors at $14° \leq \theta_{lab} \leq 25°$ for $E/A \geq 40$ MeV was not available.
[22] C. Cavata *et al.*, Phys. Rev. C **42**, 1760 (1990).
[23] Y. D. Kim *et al.*, Phys. Rev. C **45**, 338 (1992).
[24] U. Milkau *et al.*, Z. Phys. **A346**, 227 (1993).
[25] L. Phair *et al.*, Nucl. Phys. **A548**, 489 (1992).
[26] R. Trockel, Prog. Part. Nucl. Phys. **15**, 225 (1985).
[27] L. D. Landau and E. M. Lifshitz, *Statistical Physics* (Pergammon Press, New York, 1980), 3rd ed., Pt. 1.
[28] Azimuthal averaging can be neglected for the participant source ($i = 1$) because its source velocity is directed along the beam and in special cases for the spectator sources ($i = 2, 3$) when one is dealing with triple differential cross sections where the azimuthal orientation of the reaction plane is known.
[29] W. C. Hsi (to be published).
[30] W. K. Wilson *et al.*, Phys. Rev. C **45**, 738 (1992).
[31] M. B. Tsang *et al.*, Phys. Rev. C **47**, 2717 (1993).